

# PHYSICAL REVIEW B

## CONDENSED MATTER

THIRD SERIES, VOLUME 51, NUMBER 4

15 JANUARY 1995-II

### Suppression of the metal-to-insulator transition in $\text{BaVS}_3$ with pressure

T. Graf, D. Mandrus, J. M. Lawrence,\* J. D. Thompson, and P. C. Canfield<sup>†</sup>  
*Los Alamos National Laboratory, Los Alamos, New Mexico 87545*

S.-W. Cheong and L. W. Rupp, Jr.

*AT&T Bell Laboratories, Murray Hill, New Jersey 07974*

(Received 11 April 1994; revised manuscript received 31 May 1994)

The pressure dependence of the metal-to-insulator (MI) transition in  $\text{BaVS}_3$  has been studied up to applied hydrostatic pressures of 16 kbar. There is a substantial decrease in the transition temperature, with 14.8 kbar suppressing  $T_{\text{MI}}$  from 69 K at ambient pressure to about 12 K. This behavior is discussed on the basis of the crystal structure of this quasi-one-dimensional compound. We argue that the ratio of the lattice constants parallel and perpendicular to the vanadium chains is the key parameter for understanding the pressure dependence of the MI transition. Thermal-expansion and magnetization measurements at ambient pressure show no additional phase transition below 69 K. Our results indicate that the metal-to-insulator transition may be a continuous isomorphic transition from the insulator with low susceptibility due to a gap in a band of extended states to a metal with a Curie-Weiss susceptibility due to correlations in the vanadium  $d$  band.

#### I. INTRODUCTION

$\text{BaVS}_3$  has a  $P6_3/mmc$  hexagonal crystal structure at room temperature with the barium and sulfur atoms forming nearly close-packed layers perpendicular to the  $c$  axis.<sup>1</sup> The vanadium cations occupy octahedral sites enclosed by six nearest sulfur anions. The octahedra are elongated along the  $c$  axis and are face sharing, allowing the direct overlap of vanadium  $d$  orbitals with a  $\text{V}^{4+}-\text{V}^{4+}$  intrachain distance of 2.81 Å compared to 2.61 Å in vanadium metal. The direct interaction between the vanadium ions along the  $c$  axis and the large separation of the V chains of 6.73 Å (Ref. 2) strongly influence the electronic and magnetic properties of this compound.  $\text{BaVS}_3$  undergoes a second-order structural phase transition at about  $T_S=250$  K, where the symmetry is lowered from hexagonal to orthorhombic.<sup>1,3</sup> Below this temperature the dynamically disordered zigzag of the vanadium ions [observed via anisotropic thermal parameters above  $T_S$  (Refs. 2, 4, and 5)] becomes static and ordered parallel to the  $c$  axis. The point symmetry of the vanadium atoms changes from  $\bar{3}$  to  $m$  in the orthorhombic phase. No change of physical properties other than structure has been reported to occur at the transition temperature  $T_S$ . The orthorhombic splitting  $d=a_0-(b_0/\sqrt{3})$  increases continuously with decreasing temperature from 0 at 250

K to 0.13 Å at 80 K, where a sudden change of slope has been observed. This has been interpreted as a first-order phase transition, including a volume change of 0.089%.<sup>4</sup> The V-V intrachain distance in the orthorhombic phase of 2.84 Å, however, seems not to be related to the orthorhombic splitting and remains constant down to 5 K.<sup>2</sup> The space symmetry of the orthorhombic phase is  $Cmc2_1$  for all temperatures between 250 and 5 K.<sup>2,4</sup>

At high temperatures, stoichiometric  $\text{BaVS}_3$  behaves as a poor metal with a room-temperature resistivity of a few  $\text{m}\Omega\text{cm}$ . The resistivity versus temperature shows a minimum at about 130 K and a steep increase below  $T_{\text{MI}}=80$  K,<sup>1</sup> where a metal-to-insulator (MI) transition takes place. The logarithmic resistivity shows an inflection at about 40 K in sintered powder,<sup>3,6</sup> and a pronounced plateau in single crystals with current  $I\parallel c$ .<sup>7</sup> The metal-to-insulator transition has been associated with a magnetic transition. In particular, Takano<sup>3</sup> and Massenet *et al.*<sup>6</sup> observed a peak in the magnetic susceptibility at 70 K, and interpreted the peak as the onset of antiferromagnetic ordering. Inelastic spin-flip scattering of neutrons in  $\text{BaVS}_3$  showed no evidence of magnetic order on the V sites for  $31 < T < 70$  K, but showed magnetic order below 31 K where less than half of the  $\text{V}^{4+}$  sites seem to be magnetically ordered at low temperature.<sup>8</sup> Similarly, Nishihara and Takano<sup>8,9</sup> concluded from NMR measurements that no magnetic order occurs between 74 and 35

K, but that order occurs below 35 K. They interpreted the decrease of susceptibility below 74 K as due to a gradual formation of nonmagnetic pairs of V atoms, comprising 81% of the total. These authors associate the two inequivalent sites observed in the spin-echo spectrum at 1.3 K, with the remaining 19% nonpaired vanadium ions which order (antiferro)magnetically below 35 K. However, no reflections of magnetic origin, either sharp or diffuse, have been detected down to 5 K by neutron powder diffraction.<sup>2</sup> Therefore, the magnetic transition at 31–35 K is either not long range or is due to ordering of moments sufficiently small that they cannot be detected by neutron diffraction. In addition, profile refinements of neutron diffraction data as well as powder x-ray-diffraction experiments are not consistent with pairing of vanadium ions below 70 K, even short range.<sup>2,4</sup> In view of these observations, it is difficult to understand the NMR and inelastic neutron-scattering results which suggest structurally inequivalent V sites and magnetic ordering.

The Seebeck coefficient of BaVS<sub>3</sub> at 300 K is about  $-50 \mu\text{V}/\text{K}$ .<sup>1</sup> It changes sign at 70 K and increases below this temperature.<sup>10</sup> This indicates that the majority of the charge carriers are holes below the metal-to-insulator transition. Massenet *et al.*<sup>7</sup> proposed a two-band model comprising a narrow  $e(t_{2g})$  band responsible for the paramagnetic behavior of the metallic phase and centered on the large conduction band formed by the  $d_{z^2}$  orbitals. The Fermi level is situated close to the bottom of the  $e(t_{2g})$  band. This model can explain the electronic and magnetic properties of BaVS<sub>3</sub> at high temperature, but it is not compatible with the photoelectron spectroscopy studies by Itti *et al.*<sup>11</sup> This group observed a very low density of states at the Fermi level at room temperature which is in contrast to what one would expect from the above model. Examination of the Fermi edge in their ultraviolet photoemission spectroscopy (UPS) spectrum, however, suggests that the resolution may be poorer than the 0.15 eV which the authors claim. Assuming a somewhat poorer resolution could accommodate Massenet's model. The x-ray photoemission spectroscopy (XPS) data suggest further that the actual valence state of the elements in BaVS<sub>3</sub> is between 3+ and 4+ for vanadium, more than 2+ for barium, and less than 2- for sulfur. As a consequence, the vanadium  $d$  orbital contains more than one electron.

Although the sulfur stoichiometry drastically affects the electronic and magnetic behavior of the samples,<sup>6</sup> it can only in some cases explain the disagreement between different observations. From previous work, two major issues remain unresolved: the nature of the MI transition in BaVS<sub>3</sub>, and whether there are additional phase transitions below  $T_{\text{MI}}$ . To help clarify controversies surrounding these questions, we have performed magnetic-susceptibility and thermal-expansion measurements at ambient pressure as well as resistance measurements under hydrostatic pressure. Our samples are polycrystalline BaVS<sub>3</sub>, which tend to be purer<sup>1</sup> than single crystals grown from BaCl<sub>2</sub> flux. In the following sections we present and discuss results of our measurements in more detail.

## II. EXPERIMENT

High-purity powders of BaCO<sub>3</sub> and V<sub>2</sub>O<sub>5</sub> were mixed, pressed into pellets, and calcined at 650°C for 10 h in a H<sub>2</sub>S gas flow. The pellets were ground, repelletized, and sintered at 900°C for 24 h, again in a H<sub>2</sub>S gas flow. The specimens were cooled at the rate of 20°C per hour after the final sintering. X-ray analysis at room temperature showed that our samples were phase pure to a detection limit of 1% for a single impurity. A determination of the hexagonal cell parameters yielded the values  $a = 6.714(10) \text{ \AA}$  and  $c = 5.610(10) \text{ \AA}$ . The magnetic susceptibility was measured with a superconducting quantum interference device (SQUID) magnetometer (Quantum Design), and electrical resistivity was measured using a four-lead ac resistance bridge (LR-400) operating at 17 Hz. Platinum leads were attached with silver paint to the sample, which had dimensions of  $3 \times 2 \times 0.5 \text{ mm}^3$ . Cooling and warming rates during the measurement of the electrical resistivity were typically 1 K per minute. Since the sample was a polycrystalline pellet, the absolute value of the resistivity is only reliable to within roughly 20%. Hydrostatic pressures were applied using a self-clamping cell with C<sub>6</sub>F<sub>12</sub> (Fluorinert FC-75) as the pressure medium. The pressure was determined at low temperatures from the shift in the superconducting transition of high-purity lead. Corrections were made for the known temperature dependence of the pressure in this cell<sup>12</sup> when estimating the pressure dependence of high-temperature parameters. Thermal expansion was measured with a capacitance dilatometer<sup>13</sup> after faces of the pellet were polished to be parallel to each other.

## III. RESULTS

### A. Ambient pressure measurements

The resistivity as a function of temperature is compared to the susceptibility in Fig. 1. The inset focuses on the temperature range where the behavior of BaVS<sub>3</sub> is metallic. The existence of a well-defined minimum in  $\rho(T)$  at 147 K indicates the high quality of the sample studied here.<sup>1</sup> The high-temperature structural transition  $T_S = 242 \text{ K}$  manifests itself by a change in slope  $\partial\rho/\partial T$  and is indicated with a circle in the inset of Fig. 1. This value of  $T_S$  agrees well with that determined by x-ray diffraction.<sup>3,4,6,14</sup> The susceptibility follows a Curie-Weiss law between 90 and 200 K, with slight deviations from it between 200 and 350 K. In particular, no anomaly can be detected at the temperature of the hexagonal-to-orthorhombic transition. The Curie constant  $C$  obtained by fitting the data to the formula  $\chi = C/(T + \Theta)$  between 90 and 200 K is 0.22 emu/mole, which corresponds to an effective magnetic moment of  $p_{\text{eff}} = 1.33\mu_B$ , and  $\Theta = -9 \text{ K}$ . The effective magnetic moment  $p_{\text{eff}}$  is somewhat greater than the values reported in the literature [ $p_{\text{eff}} = 1.17\mu_B$ ,<sup>6</sup>  $1.2\mu_B$ ,<sup>9</sup>  $1.27\mu_B$  (Ref. 10)] but still is significantly smaller than  $1.73\mu_B$  expected for a spin- $\frac{1}{2}$  localized on each V<sup>4+</sup> ion. This reduced  $p_{\text{eff}}$  has been attributed to the existence of delocalized electrons in the  $d_{z^2}$  band which contributes very little to the magnetic sus-

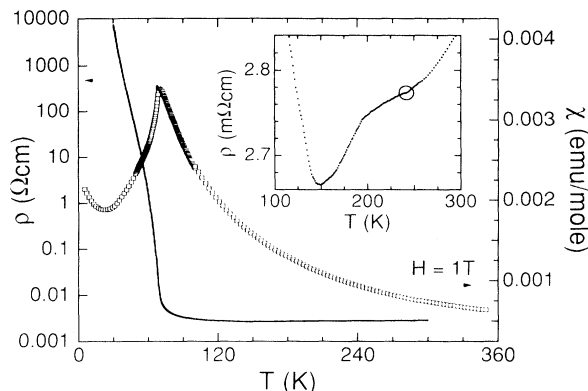


FIG. 1. Resistivity (solid line, left axis) and magnetic susceptibility at a field of 1 T (open squares, right axis) as a function of temperature. Both measurements are at ambient pressure. Inset: Resistivity at 1 bar and high temperature. The circle shows where the structural transition occurs.

ceptibility.<sup>7</sup> From measuring several different samples we found that a smaller  $p_{\text{eff}}$  is also associated with samples having a lower sulfur content. Massenet *et al.*<sup>6</sup> showed that  $T_S$  is suppressed from 240 K for  $\text{BaVS}_{2.97 \pm 0.03}$  to 150 K for  $\text{BaVS}_{2.88 \pm 0.03}$  and Gardner, Vlasse, and Wold<sup>1</sup> measured a positive temperature-dependent resistivity of a sample found to be stoichiometric by chemical analysis. Given our observation of  $T_S = 242$  K and of metallic resistivity, we believe our sample is nearly stoichiometric.

The magnetic susceptibility and the thermal expansion vs temperature are plotted in Fig. 2(a) and the thermal-

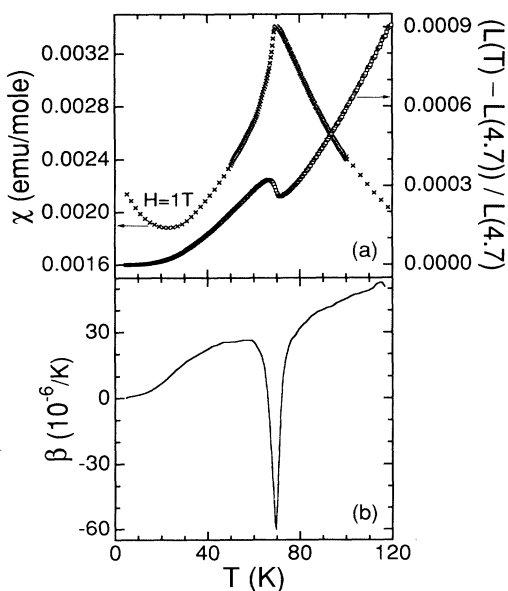


FIG. 2. (a) Temperature dependence of the magnetic susceptibility at a field of 1 T (crosses, left axis) and the linear thermal expansion (open squares, right axis). Both curves are taken on warming the sample at ambient pressure. (b) Thermal expansion coefficient  $\beta = (3/L)(\partial L/\partial T)$  as a function of temperature.

expansion coefficient  $\beta = (1/V)(\partial V/\partial T)$ , which for polycrystalline samples should be equivalent to  $(3/L)(\partial L/\partial T)$ , is shown in Fig. 2(b), also as a function of temperature. A transition is observed centered at 69.2 K which nearly coincides with the maximum of the magnetic susceptibility at 70 K. Differences in the transition temperature of 0.3 K between cooling and warming data (for cooling and warming rates varying between 2 and 6 K per hour) can more probably be attributed to the thermometry than to intrinsic hysteresis. A slight volume contraction can be observed upon heating the specimen through the transition. We obtained for the volume change the value  $\Delta V/V = 3\Delta L/L = 0.019\%$  by simply subtracting the value of  $L$  at the local minimum from that at the local maximum. A value of 0.04% was obtained by extrapolating both the high- and low-temperature data to 69.2 K. Comparison of our data with the low-temperature x-ray measurements of Sayetat *et al.*<sup>4</sup> is very intriguing. These authors found a positive volume change of 0.089% upon heating. The resolution for the length change of our experiment is higher than with x-ray diffractometers ( $\Delta L/L = 10^{-7}$  compared to  $3 \times 10^{-5}$  relative resolution<sup>4</sup>), but we determine the thermal expansion of the bulk sample containing pores, grain boundaries, etc. To rule out a sign error due to preferential orientation, we measured the sample a second time but rotated by 90°. The two curves are identical. As we will discuss further below, our observation of a volume contraction on warming is consistent with the pressure dependence of  $T_{\text{MI}}$ .

A minimum in the magnetic susceptibility occurs at 23 K. In past work, this minimum was observed to be correlated with the inflection in  $\log(\rho(T))$ , and was believed to signal the onset of a third phase transition.<sup>10</sup> We observed, however, that the low-temperature tail and the temperature of the minimum in the susceptibility curve are considerably sample dependent, and furthermore that the inflection in  $\log(\rho(T))$  of the sample presented here does not correlate with the minimum in the susceptibility but occurs near 45 K. Isothermal magnetization measurements on our sample at 5, 40, and 80 K indicate the presence of a ferromagnetic contribution to the susceptibility which is barely detectable at 80 K. In addition, we observed hysteretic behavior of the Curie tail below 15 K when the susceptibility was measured in fields of 100 and 500 G. We believe that the gradual (and irreproducible) increase of  $\chi(T)$  below 23 K, the ferromagnetic contribution, and the hysteresis reflect the presence of a second phase (possibly sulfur deficient), rather than a phase transition. If we assume that the second phase has a saturated moment comparable to that reported by Massenet *et al.*,<sup>7</sup> then our sample contains less than 1% of this phase. Finally, we note that aging at room temperature does not modify the sulfur content of the samples. We obtained an identical  $\chi(T)$  curve one year after the first measurements.

## B. Pressure dependence of the phase transitions

Figure 3 shows the electrical resistivity for  $\text{BaVS}_3$  at four applied pressures as a function of temperature taken

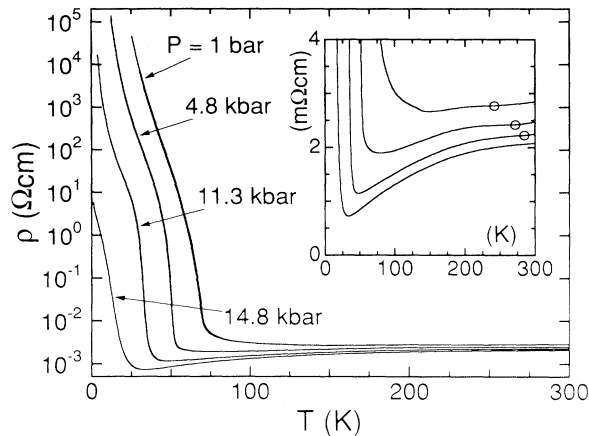


FIG. 3. Temperature dependence of the resistivity of BaVS<sub>3</sub> under various hydrostatic pressures. Values of  $P$  indicated are those at low temperature, determined by the superconducting transition of lead. Each data set represents cooling and warming curves; hysteresis is negligible. Inset:  $\rho(T)$  upon cooling at the same applied pressures shown on a limited resistivity scale. Near room temperature the pressure is higher than at low temperatures, as explained in the text. The circles indicate the change of slope due to the hexagonal-to-orthorhombic transition.

on cooling and warming the sample. As mentioned earlier, the high-temperature structural transition  $T_S$  can be identified by a weak change of the slope  $\partial\rho/\partial T$  near 250 K. Circles in the inset of Fig. 3 mark this transition. The hexagonal-to-orthorhombic transition occurs at 242 K under ambient pressure and increases with increasing pressure to 272 K at 7 kbar, 285 K at 13.1 kbar, and to over 300 K at  $P > 16$  kbar. (Note that these pressure values differ from those indicated in Fig. 3 because they have been corrected for the temperature variation of pressure in our cell,<sup>12</sup> which causes the pressure to be higher at higher temperatures.) Although not obvious in the inset of Fig. 3, the change of slope at the transition becomes more pronounced at high pressure. The room-temperature resistivity for the different pressures is between 2.1 and 2.9 mΩ cm, which is slightly lower than the value originally reported by Gardner, Vlasse, and Wold.<sup>1</sup> The samples become better metals with increasing pressure, as evidenced by an increase in  $\partial\rho/\partial T$ . Extrapolated residual resistivity ratios  $\rho(300)/\rho(0)$  vary from 1.2 at 1 bar to roughly 8 at 14.8 kbar. Below the metal-to-insulator transition the log of the resistivity increases monotonically as shown in Fig. 3, and has an inflection at a temperature well below  $T_{MI}(P)$ . Figure 4 plots the logarithmic derivative of the temperature-dependent resistivity (cooling and heating data). The peaks provide a means of defining the value of  $T_{MI}$ ,<sup>15</sup> as opposed to simple inspection of the  $\rho(T)$  plot. The transition is sharper for the intermediate pressures, which is manifested in the width of the peak in  $(1/\rho)(\partial\rho/\partial T)$ . As pressure is increased,  $T_{MI}$  decreases, which is opposite to the evolution of  $T_S(P)$ . A small hysteresis of about 1.5 K can be detected for the 1-bar data below 75 K. We have established that this behavior is not intrinsic but is due to

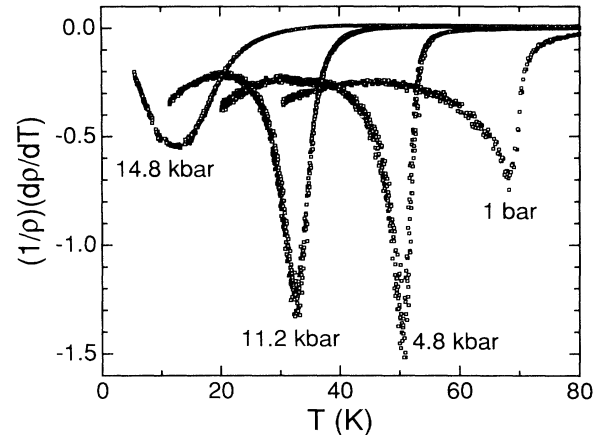


FIG. 4. Logarithmic derivative of the temperature dependent resistivity of BaVS<sub>3</sub> under hydrostatic pressure. The pressure values indicated are corrected at the MI transition temperature.

a small thermal gradient between the thermometer and the sample which subsequently was minimized. Plots of  $\ln(\rho)$  vs  $1/T$  (characteristic of a semiconducting gap, impurity level, or thermally activated hopping) or  $1/T^{1/4}$  (such as found for variable range hopping<sup>16</sup>) have no significant region of linearity. However, a temperature-dependent activation energy can be estimated from the formula  $\rho = \rho_\infty \exp(\Delta/T)$  to be  $\Delta \approx 560$  K at 25 K and ambient pressure (see below). The evolution of the metal-to-insulator transition as a function of pressure is shown in Fig. 5. The sensitivity of  $T_{MI}$  to pressure is  $-3.4$  K/kbar, on average, and a linear extrapolation suggests that the MI transition would be totally suppressed at 20 kbar. Hints for a total suppression can already be detected in Figs. 3 and 4. The MI transition clearly broadens under 14.8 kbar and the resistivity increase below  $T_{MI}$  is smaller than at lower pressure. A negative pressure derivative of  $T_{MI}$  also follows from the thermal-expansion change  $\Delta\beta$  at  $T_{MI}$  [Fig. 2(b)] and Ehrenfest's relation for a second-order phase transition,  $dT_c/dP = VT_c \Delta\beta/\Delta C$ . Because  $\Delta C$  must be positive at

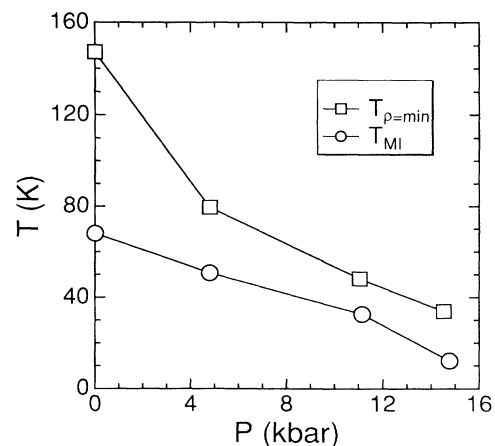


FIG. 5. Pressure dependence of  $T_{MI}$  and  $T(\rho=\min)$ .

the transition,  $dT_c/dP$  must be negative. (This result provides further support for our finding that the volume change on cooling through  $T_{MI}$  is positive.) The temperature of the minimum in resistivity is also plotted as a function of pressure in Fig. 5.  $T(\rho=\min)$  decreases with increasing pressure from 147 K at 1 bar to 34 K at 14.8 kbar. The value of the resistivity at the minimum also decreases.

#### IV. DISCUSSION

The metallic behavior at high temperature, the large magnetic moment associated with the existence of the Curie-Weiss law above 90 K, and the weak increase of  $\chi(T)$  below 20 K [Figs. 1 and 2(a)] indicate that the sample studied is close to stoichiometric  $BaVS_3$ .<sup>1,6</sup> From Figs. 2(b) and 4 we estimate a transition width of 8 K for the metal-to-insulator transition, which we believe to be intrinsic and which attests further to the high quality of this sample.

With applied pressure the MI transition drops rapidly to lower temperatures, while the high-temperature structural transition moves up. These trends can be interpreted by considering the ratio of lattice parameters  $c/a$ , where  $c$  is the lattice parameter along the  $V$ -chain direction, and  $a$  is the hexagonal basal plane lattice constant that is related to the orthorhombic cell parameters by  $a=(a_0b_0/\sqrt{3})^{1/2}$ , as shown by the inset in Fig. 6. The main part of Fig. 6 shows that experimentally this ratio is always greater than the value 0.8165 that corresponds to perfect octahedral symmetry of the six sulfur ions surrounding a vanadium cation,<sup>4,7</sup> so that the measured  $c/a$  ratios reflect the distortion of the octahedra. The  $c/a$  ratio increases with decreasing temperature in the hexagonal phase to a critical value at the structural transition at 242 K. Below this temperature the tempera-

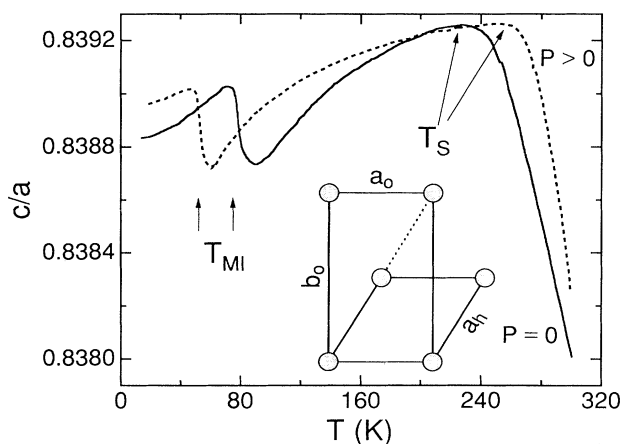


FIG. 6. Evolution of the ratio  $c/a$  with temperature. This ratio is taken as  $c_h/a_h$  and  $c_0(a_0b_0/\sqrt{3})^{1/2}$  for hexagonal and orthorhombic symmetries, respectively. The solid line is x-ray data at ambient pressure from Ref. 4; the dashed line is the proposed behavior under pressure (see text). Also shown is the vanadium sublattice in the  $ab$  plane with the crystallographic unit cells outlined.

ture dependence of  $c/a$  changes sign, and decreases on cooling to a critical value where the MI transition sets in. A reasonable expectation is that application of hydrostatic pressure should increase  $c/a$  due to anisotropic compression parallel and perpendicular to the vanadium chains. This can be understood by simple inspection of the crystal structure with its strong metallic bonds along the  $c$  axis, which should be relatively incompressible, or by the anisotropy of the thermal vibrations of the vanadium atoms.<sup>2,4,5</sup> Since pressure increases  $c/a$ , the critical value needed for the hexagonal-to-orthorhombic transition is reached at a higher temperature, i.e., pressure pushes the maximum in  $c/a$  and  $T_S$  to higher temperatures, as observed by experiment (inset of Fig. 3). By the same mechanism, applied pressure weakens the decrease of  $c/a(T)$  in the orthorhombic phase and  $T_{MI}$  shifts to lower temperature (see dashed line in Fig. 6). The more metallic behavior of  $BaVS_3$  under pressure then would be due predominantly to the slightly better overlap of the vanadium  $d$  orbitals along the  $c$  axis.

We consider next the issue of whether a third, magnetic phase transition occurs at low temperatures (below 35 K). The monotonic evolution of the thermal expansion between 4.7 and 60 K is a sensitive indication for the absence of such a phase transition in this temperature range.  $\beta(T)$  varies according to the Debye function without any anomaly below 60 K (Fig. 2). We argued above that the (irreproducible) Curie tail in the susceptibility and the associated small remnant magnetization and hysteresis reflect the existence of a second phase (presumably sulfur deficient) comprising at most 1% of the sample, rather than an intrinsic phase transition. However, we note that the onset at 31 K of a magnetic phase transition in  $BaVS_3$  found by Heidemann and Takano<sup>8</sup> is within the temperature range where we observed susceptibility minima on different samples. In addition, Massenet *et al.*<sup>7</sup> reported ferromagnetic order only below 20 K in their sulfur-deficient single crystal, whereas we detected a (small) remnant magnetization at substantially higher temperatures. Given these caveats, we cannot identify unambiguously the source of the ferromagnetic contribution to the susceptibility observed in our sample.

Finally, we turn to the nature and the order of the transition at  $T_{MI}$ . As discussed in Sec. I, the maximum of the susceptibility at 70 K was originally taken to represent the onset of antiferromagnetic order, but later studies showed, at least between 35 and 70 K, that there is no hyperfine field in NMR,<sup>9</sup> Mössbauer,<sup>6</sup> or neutron spin-flip scattering,<sup>8</sup> and no magnetic reflections in neutron diffraction.<sup>2</sup> Although it is possible that order takes place, but with an ordered moment too small to be detectable by these measurements (e.g.,  $\mu_{ord} \ll 0.1\mu_B$ ), this seems unlikely since small-moment order should not give rise to such a large reduction in the susceptibility below  $T_{MI}$ . This quandary led to speculations that some form of one-dimensional (1D) antiferromagnetism occurs along the vanadium chains, e.g., the suggestion<sup>9</sup> that non-magnetic  $V$  pairs form gradually below  $T_{MI}$ . The negative slope  $\partial\rho/\partial T$  which can be observed in the wide temperature range between  $T_{MI}$  and the temperature  $T_{min}$  of the

resistivity minimum might be attributed to fluctuations in the order parameter above  $T_{\text{MI}}$ , as is commonly found in low-dimensional phase transitions. A problem with this interpretation is that such 1D order is typically unstable against structural pairing, and no such pairing is detected in neutron or x-ray crystallography.<sup>2,4</sup> Furthermore, examination of Fig. 2(a) shows that the decrease in  $\chi(T)$  on cooling below 70 K is more rapid than occurs in typical examples of 1D antiferromagnetic compounds or in the predictions from 1D antiferromagnetic models.<sup>17</sup>

We propose an alternate explanation. Not only is no magnetic order detected below  $T_{\text{MI}}$ , but also no crystallographic change is observed by x-ray or neutron diffraction.<sup>2,4</sup> It could be that these experiments have not been sufficiently sensitive to resolve symmetry breaking; however, it is also possible that symmetry above and below  $T_{\text{MI}}$  is not broken. This suggests that the transition is *isomorphic*, i.e., there is no symmetry change, but only a change in cell volume, which is the order parameter for the transition. An isomorphic transition has been found for certain  $\text{RNiO}_3$  compounds ( $R$  = rare earth). These are “charge transfer” compounds, growing in a modified perovskite structure, where the MI transition is accompanied by a 0.2% contraction of the unit cell on heating into the metallic state.<sup>18</sup> (The volume contraction at  $T_{\text{MI}}$  in these oxides and in  $\text{BaVS}_3$  is linked to electronic delocalization, i.e., metallic bonding.) For  $R = \text{Pr}$  and  $\text{Nd}$  there is no structural symmetry change, but the insulating phase is antiferromagnetic.<sup>18</sup> For  $R = \text{Sm}$  and  $\text{Eu}$ , however, the MI transition is not accompanied by *any* breaking of symmetry, structural or magnetic. The magnetic transition which occurs does so at a lower temperature than  $T_{\text{MI}}$ .<sup>19</sup> The qualitative shape of the logarithmic resistivity in  $\text{BaVS}_3$  is very similar to that of these compounds, but the features in the latter are more pronounced. In particular, the plateau below the jump in  $\log(\rho(T))$  associated with the MI transition is very extended in  $\text{RNiO}_3$ . Hence, except for the fact that the MI transition in  $\text{RNiO}_3$  is clearly first order and hysteretic,<sup>20</sup> we argue that the MI transition in  $\text{BaVS}_3$  is similar to that of  $\text{SmNiO}_3$  or  $\text{EuNiO}_3$ , i.e., isomorphic, but this is not to say that  $\text{BaVS}_3$  is a charge-transfer system.

This brings us to the question of the order of the transition. In examples of isomorphic transitions such as the  $\alpha$ - $\gamma$  valence transition in elemental cerium<sup>21</sup> or the metal-to-insulator transition in  $\text{V}_{2-x}\text{Cr}_x\text{O}_3$ ,<sup>22</sup> a line of transitions in the  $P$ - $T$  or  $x$ - $T$  plane terminates at a critical point, beyond which the transitions become continuous with rapid changes in thermodynamic quantities as functions of temperature, but no true divergences. We argue that the MI transition in  $\text{BaVS}_3$  can be viewed as a continuous transition that is taking place at ambient pressure just beyond a first-order critical point as occurs for  $x = 0.005$  in  $\text{V}_{2-x}\text{Cr}_x\text{O}_3$ . Our reasons are as follows: First of all, unlike the case of  $\text{RNiO}_3$ , we observe no intrinsic hysteresis in the resistivity, susceptibility, or thermal expansion. Furthermore, the volume change is much smaller in  $\text{BaVS}_3$  (0.02%) than in the oxides (where it is 0.2%). Such a small change would indicate that even if the transition were first order, it would be very close to

a critical point where the discontinuity in  $\Delta V$  vanishes. The third observation is the very broad peak in  $(1/\rho)$  ( $\partial\rho/\partial T$ ) for  $P = 14.8$  kbar (Fig. 4). The shape of this curve suggests a continuous transition from the metallic to insulating states, and the trends shown in Fig. 4 evidence that pressure moves  $\text{BaVS}_3$  away from a well-defined transition. Fourth, the broad region of negative  $\partial\rho/\partial T$  observed between  $T_{\text{MI}}$  and  $T_{\text{min}}$  for all pressures could not occur for a strong first-order transition. This can be seen by comparison to the first-order transition in  $\text{RNiO}_3$ , where the resistivity in the metallic region is monotonically increasing for all pressures.<sup>20</sup> The negative  $\partial\rho/\partial T$  in  $\text{BaVS}_3$  rather indicates a continuous transition of the order parameter above  $T_{\text{MI}}$ . Finally, we have attempted an analysis of the critical behavior of the thermal expansion which implies that the transition is continuous. To accomplish this, we first estimate the background thermal expansion by fitting the measured expansion  $L_{\text{meas}}$  [solid line, Fig. 7(a) inset] to a single polynomial  $L_{\text{back}}$  (dashed line, inset) whose temperature dependence is the same as that of the measured data well away from the transition region. Subtracting to obtain  $L_{\text{crit}} = L_{\text{meas}} - L_{\text{back}}$ , we then plot  $\Delta L_{\text{crit}} = L_{\text{crit}}(T)$

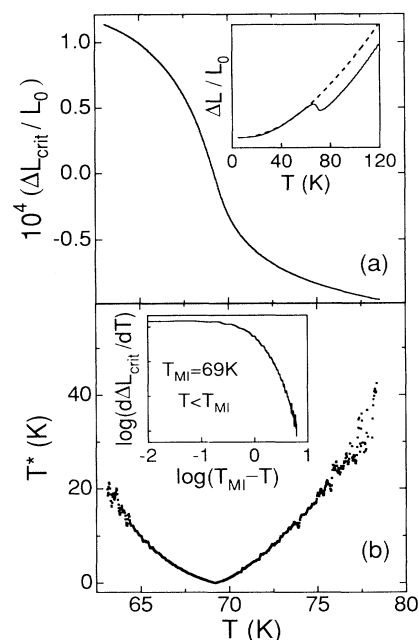


FIG. 7. (a) Critical behavior  $\Delta L_{\text{crit}}/L_0$  of the thermal expansion near  $T_{\text{MI}}$ . The dashed line in the inset represents our estimate of the background thermal expansion, which was subtracted from the measured expansion (solid line, inset) to obtain  $L_{\text{crit}}$ . (See text for details.) (b) The quantity  $T^*(T) \equiv \Delta L_{\text{crit}}/(\partial L/\partial T)$  plotted vs temperature. This has the appearance expected for an isomorphic transition located on the continuous side of a critical point (see text). Inset:  $\log(\Delta L_{\text{crit}}/\partial T)$  vs  $\log(T - T_{\text{MI}})$ . The tick marks of the y axis are separated by 0.3. The lack of linearity is as expected for a continuous transition, as opposed to a first-order transition or a transition through a critical point terminating a line of first-order transitions.

$-L_{\text{crit}}(T_{\text{MI}})$  in Fig 7(a). Assuming that  $\Delta L_{\text{crit}}/L_0$  varies as  $|\varepsilon|^\delta$  [where  $\varepsilon=(T-T_{\text{MI}})/T_{\text{MI}}$  and  $L_0=L(4.7\text{ K})$ ], in Fig 7(b) we show the quantity

$$T^*(T) = \left| \Delta L_{\text{crit}} / \left[ \frac{\partial \Delta L_{\text{crit}}}{\partial T} \right] \right|,$$

which should vary as  $|T-T_{\text{MI}}|/\delta$  above and below the transition. We also plot [inset to Fig. 7(b)]  $\log(\partial \Delta L_{\text{crit}}/\partial T)$  vs  $\log(T-T_{\text{MI}})$ , which should yield a straight line with slope  $\delta-1$ . For second-order symmetry-changing transitions or for an isomorphous transition at a critical point, these plots are typically linear over an extended range  $0.001 < \varepsilon < 0.1$ .<sup>21</sup> In Fig. 7(b), no region of linearity is visible for the two ways of plotting the data. [In these plots we have fixed  $T_{\text{MI}}$  as the temperature of the maximum thermal expansion; other choices of  $T_{\text{MI}}$  give asymmetrical curves in Figs. 7(a) and 7(b). The absence of linearity holds independent of choice of  $T_{\text{MI}}$  and, as can be seen from Fig. 7(b), is not an artifact of the statistics.] Indeed, the  $T^*$  curve is similar to those for  $\text{Ce}_{1-x}\text{Th}_x$  alloys which have continuous isomorphous valence transitions for  $x > x_c$ .<sup>21</sup> It can already be seen from Fig. 7(a) that there is no divergence in slope of  $\Delta L_{\text{crit}}$  at  $T_{\text{MI}}$ . For these five reasons we assert that the transition is not first order or critical, but is continuous.

A continuous MI transition is not without precedent. We have already mentioned the case of Cr-doped  $\text{V}_2\text{O}_3$ .<sup>22</sup> Other examples are the MI transitions in FeSi and in the recently discovered ‘‘Kondo insulator’’  $\text{Ce}_3\text{Bi}_4\text{Pt}_3$ .<sup>23</sup> In these latter compounds optical conductivity experiments<sup>24,25</sup> suggest that the semiconducting gap ‘‘renormalizes’’ (i.e., vanishes) continuously as the temperature is raised. In Fig. 8 we use a simple model [where two wide, equal mass, parabolic bands are separated by a temperature-dependent gap  $\Delta(T)$  and the scattering rate is assumed linear with temperature, i.e., electron-phonon scattering dominates] to estimate the temperature dependence of the gap in  $\text{BaVS}_3$  from the resistivity data. The model has been applied by Hundley *et al.* to  $\text{Ce}_3\text{Bi}_4\text{Pt}_3$ .<sup>26</sup> The energy gap  $\Delta$  obtained from this model is essentially

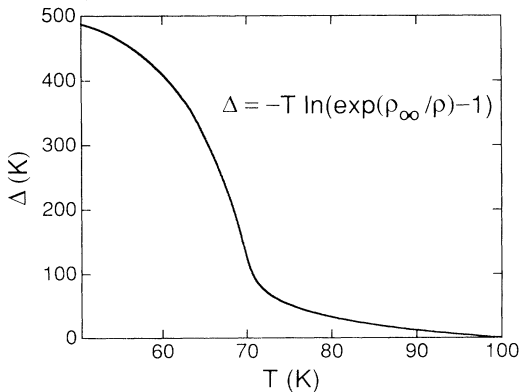


FIG. 8. The temperature dependence of the gap, estimated from the resistivity using the model of Hundley *et al.* (Ref. 26):  $\Delta = -T \ln[\exp(\rho_\infty/\rho) - 1]$ . The gap renormalizes continuously to zero as temperature increases.

the same as the one calculated with the formula  $\rho \sim \rho_\infty \exp(\Delta/T)$ , except at higher temperature ( $T > 70\text{ K}$ ). Given the uncertainty in  $\rho_\infty$ , the resistivity in the limit of very high temperatures, and the simplicity of the model, the curve of Fig. 8 has only qualitative significance. It is merely intended to reinforce the analogy to FeSi and  $\text{Ce}_3\text{Bi}_4\text{Pt}_3$  and to suggest that the physics of the transition in  $\text{BaVS}_3$  involves a continuous renormalization of the gap.

In FeSi the susceptibility is small at low temperature due to the presence of a gap in a (highly correlated)  $d$  band of extended states. At high temperatures the susceptibility exhibits Curie-Weiss behavior<sup>27</sup> which arises from strong Coulomb correlations in the  $3d$  band.<sup>28</sup> For  $\text{BaVS}_3$  the behavior of  $\chi(T)$  can be understood in a similar way. The fact that the peak at  $T_{\text{MI}}$  is much sharper than in FeSi is consistent with  $\text{BaVS}_3$  being closer to a critical point. Figure 9 compares the derivative of  $T\chi(T)$  with the derivative  $-\partial(\log\rho)/\partial T$ . Both curves peak at 69 K and have similar shapes, indicating that changes in the electronic and magnetic characters are correlated strongly.<sup>15,20</sup> Combined with use of the formula  $\rho \sim \rho_\infty \exp(\Delta/T)$ , the equality of these derivatives suggests that  $T\chi \sim \Delta$  in the vicinity of  $T_{\text{MI}}$  (corrections are of the order of 10%). An identical relationship is valid for  $\text{Ce}_3\text{Bi}_4\text{Pt}_3$ ,<sup>29</sup> which strengthens the case that the susceptibility of  $\text{BaVS}_3$  can be understood in terms similar to that of FeSi and  $\text{Ce}_3\text{Bi}_4\text{Pt}_3$ .

To summarize, our argument is that the MI transition in  $\text{BaVS}_3$  is a continuous isomorphous transition, involving a smooth crossover from an insulator, with low susceptibility due to a gap in otherwise extended states and with no magnetic order, to a metal with Curie-Weiss behavior arising from strong Coulomb correlations in the vanadium  $d$  band. The gap renormalizes continuously to zero as the temperature is raised. The situation is similar in many respects to that of FeSi, but, due to close proximity to a critical point, the continuous transition is sharper.

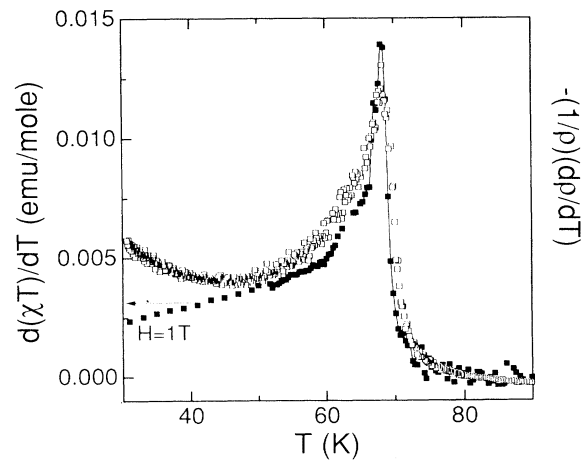


FIG. 9. Derivative of  $\chi T$  with respect to temperature (filled squares and line, on left axis), and the logarithmic derivative of the temperature-dependent resistivity (open squares, on right axis) at ambient pressure. Only warming data are shown.

This does not mean that the microscopic physics is identical to that of FeSi. For unlike that material, the physics of BaVS<sub>3</sub> clearly is determined by changes that the octahedral distortion of the quasi-1D vanadium chains have on the electron states. Indeed, the idea of Massenet *et al.*<sup>7</sup>—that above 70 K a narrow correlated  $d_{xy}$  band, responsible for the magnetic behavior, overlaps a broad  $d_{z^2}$  band, responsible for the metallic behavior—may be applicable. It requires that a gap develops continuously in the hybridized  $d$  band, and that the gap suppresses the moment at low temperature. This would be similar to the situation in Ce<sub>3</sub>Bi<sub>4</sub>Pt<sub>3</sub> where a narrow ( $4f$ ) state is degenerate with a broad band of conduction states, and a small energy gap separates a high-temperature conducting local-moment regime from a low-temperature, nonmagnetic insulator.

### V. CONCLUSION

The resistivity of stoichiometric BaVS<sub>3</sub> has been measured as a function of temperature under applied hydrostatic pressure. A pressure of 14.8 kbar suppresses the metal-to-insulator transition from 69 K at 1 bar to 12 K. The pressure dependence of this transition is correlated with changes of the ratio  $c/a$ , and we propose that the decrease of  $T_{MI}$  is due to the anisotropic compression of the unit cell. BaVS<sub>3</sub> has been studied at ambient pressure

by resistivity, magnetic-susceptibility, and thermal-expansion experiments. The measurements confirm the existence of two phase transitions, a structural one at 242 K and one from a metallic-to-insulating state at 69 K, which have opposite pressure dependencies. No evidence for an additional intrinsic phase transition between 5 and 60 K has been found. Analysis of our data suggests that the metal-to-insulator transition may be a continuous isomorphic transition from a low-moment band insulator to a metal with Curie-Weiss behavior arising from strong Coulomb correlations in the vanadium  $d$  band. Clearly, spectroscopic studies (optical conductivity, photoemission, inelastic neutron scattering) on high-quality single crystals are required to clarify the nature of the metal-to-insulator transition in BaVS<sub>3</sub>.

### ACKNOWLEDGMENTS

Work at Los Alamos was performed under the auspices of the U.S. Department of Energy. J.M.L. was supported by the Center for Materials Science at Los Alamos under the University of California Personnel Assignment Program. Ames Laboratory is operated for the U.S. Department of Energy by Iowa State University under Contract No. W-7405-ENG-82, and work there was supported by the Director of Energy Research, Office of Basic Energy Sciences.

\*Permanent address: Department of Physics, University of California, Irvine, California 92717.

†Present address: Ames Laboratory, Ames, Iowa 50011.

<sup>1</sup>R. A. Gardner, M. Vlasse, and A. Wold, *Acta Crystallogr. Sec. B* **25**, 781 (1969).

<sup>2</sup>M. Ghedira, M. Anne, J. Chenavas, M. Marezio, and F. Sayetat, *J. Phys. C* **19**, 6489 (1986).

<sup>3</sup>M. Takano, H. Kosugi, N. Nakanishi, M. Shimada, T. Wada, and M. Koizumi, *J. Phys. Soc. Jpn.* **43**, 1101 (1977).

<sup>4</sup>F. Sayetat, M. Ghedira, J. Chenavas, and M. Marezio, *J. Phys. C* **15**, 1627 (1982).

<sup>5</sup>M. Marezio, *Chem. Scr.* **26A**, 91 (1986).

<sup>6</sup>O. Massenet, R. Buder, J. J. Since, C. Schlenker, J. Mercier, J. Kelber, and D. G. Stucky, *Mater. Res. Bull.* **13**, 187 (1978).

<sup>7</sup>O. Massenet, J. J. Since, J. Mercier, M. Avignon, R. Buder, V. D. Nguyen, and J. Kelber, *J. Phys. Chem. Solids* **40**, 573 (1979).

<sup>8</sup>A. Heidemann and M. Takano, *Phys. Status Solidi B* **100**, 343 (1980).

<sup>9</sup>H. Nishihara and M. Takano, *J. Phys. Soc. Jpn.* **50**, 426 (1981).

<sup>10</sup>K. Matsuura, T. Wada, T. Nakamizo, H. Yamauchi, and S. Tanaka, *Phys. Rev. B* **43**, 13 118 (1991).

<sup>11</sup>R. Itti, T. Wada, K. Matsuura, T. Itoh, K. Ikeda, H. Yamauchi, N. Koshizuka, and S. Tanaka, *Phys. Rev. B* **44**, 2306 (1991).

<sup>12</sup>J. D. Thompson, *Rev. Sci. Instrum.* **55**, 231 (1984).

<sup>13</sup>R. Pott and R. Schefzyk, *J. Phys. E* **16**, 444 (1983).

<sup>14</sup>T. Wada, M. Shimada, and M. Koizumi, *J. Solid State Chem.* **33**, 357 (1980).

<sup>15</sup>M. E. Fisher and J. S. Langer, *Phys. Rev. Lett.* **20**, 665 (1968); Y. Suezaki and H. Mori, *Prog. Theor. Phys.* **41**, 1177 (1969).

<sup>16</sup>N. F. Mott, *Metal-Insulator Transitions* (Taylor & Francis, London, 1974), p. 34.

<sup>17</sup>L. J. DeJongh and A. R. Miedema, *Adv. Phys.* **23**, 1 (1974).

<sup>18</sup>P. Lacorre, J. B. Torrance, J. Pannetier, A. I. Nazzal, P. W. Wang, and T. C. Huang, *J. Solid State Chem.* **91**, 225 (1991).

<sup>19</sup>J. B. Torrance, P. Lacorre, A. I. Nazzal, E. J. Ansaldo, and Ch. Niedermayer, *Phys. Rev. B* **45**, 8209 (1992).

<sup>20</sup>P. C. Canfield, J. D. Thompson, S.-W. Cheong, and L. W. Rupp, *Phys. Rev. B* **47**, 12 357 (1993).

<sup>21</sup>J. M. Lawrence, P. S. Riseborough, and R. D. Parks, *Rep. Prog. Phys.* **44**, 1 (1981).

<sup>22</sup>D. B. McWhan, J. P. Remeika, T. M. Rice, W. F. Brinkman, J. P. Maita, and A. Menth, *Phys. Rev. Lett.* **27**, 941 (1971).

<sup>23</sup>M. F. Hundley, P. C. Canfield, J. D. Thompson, Z. Fisk, and J. M. Lawrence, *Phys. Rev. B* **42**, 6842 (1990).

<sup>24</sup>Z. Schlesinger, Z. Fisk, H. T. Zhang, M. B. Maple, J. F. Ditsa, and G. Aeppli, *Phys. Rev. Lett.* **71**, 1748 (1993).

<sup>25</sup>B. Bucher, Z. Schlesinger, P. C. Canfield, and Z. Fisk, *Phys. Rev. Lett.* **72**, 522 (1994).

<sup>26</sup>M. F. Hundley, P. C. Canfield, J. D. Thompson, and Z. Fisk, *Physica B* **199+200**, 443 (1994).

<sup>27</sup>K. Tajima, Y. Endoh, J. M. Fischer, and G. Shirane, *Phys. Rev. B* **38**, 6954 (1988).

<sup>28</sup>S. N. Evangelou and D. M. Edwards, *J. Phys. C* **16**, 2121 (1983).

<sup>29</sup>M. F. Hundley (private communication).